

DEFLAGRATION-TO-DETONATION TRANSITION
IN ‘GASEOUS OXYGEN – LIQUID FUEL FILM’
SYSTEM

S. M. Frolov^{1,2,3}, V. S. Aksenov^{1,2,3}, and I. O. Shamshin^{1,2,3}

¹Center for Pulsed Detonation Combustion
Moscow, Russia
e-mail: smfrol@chph.ras.ru

²N. N. Semenov Institute of Chemical Physics
Russian Academy of Sciences
Moscow, Russia

³National Research Nuclear University “MEPhI”
(Moscow Engineering Physics Institute)
Moscow, Russia

Deflagration-to-detonation transition (DDT) in a channel with gaseous oxygen in the volume and a thin film of liquid *n*-heptane on the bottom wall has been obtained experimentally at weak ignition by a source, which generates the initial shock wave (SW) of insignificant intensity. In a series of experiments with different ignition energy (14 to 480 J) in a straight 3-meter long channel of rectangular cross section 54×24 mm with smooth internal walls and with one open end, the DDT in such a stratified system was detected at run-up distances of 1 to 2 m from the ignition source and run-up time of 3.4 to 30 ms after ignition. In some experiments, a quasi-stationary low-speed detonation-like combustion front, traveling at an average velocity of 700–900 m/s was detected with the structure including a leading SW followed by a reaction zone separated by a time delay of 80 to 150 μ s.

Introduction

Due to the potential possibility of increasing the energy efficiency of aircraft propulsion systems by substituting deflagrative combustion by controlled detonative combustion, there currently exist two main

schemes of arranging detonative combustion: one with detonations continuously rotating in the annular combustor in the tangential direction (referred to as Rotating Detonation Combustor, RDC [1]) and the other with periodic detonations traveling along the combustor (referred to as Pulse Detonation Combustor, PDC [2]). The first scheme is treated as the most promising for further improvement of liquid rocket and turbojet engines, whereas the second is considered for ramjet engines designed for subsonic and supersonic flight. Liquid fuel in RDCs and PDCs is preferably supplied in the form of sprays, but it may be also fed in the form of wall films [3, 4]. To properly arrange the operation process in RDC and PDC with the feed of liquid fuel in the form of wall film it is necessary to know the propagation mechanism and properties of heterogeneous detonation in the ‘gas–film’ system, as well as the requirements for DDT and detonation initiation.

In all known experimental studies, the detonation in ‘gas–film’ system was initiated by powerful sources. Apparently, Loison [5] was the first who observed detonation in such a system in an 80–100-meter long tube of 250-millimeter diameter with the 0.1–0.3-millimeter-thick oil film deposited on internal tube walls and filled with air. The initiating pulse was generated by burning a homogeneous charge of methane–air mixture at an initial pressure of 7 bar in a 4-meter long high-pressure section separated from the main tube by a bursting diaphragm. Unlike gas detonation, which occurs near a powerful initiation source, a detonation-like blast wave in experiments [5] arose after a long transition period and propagated with an apparent velocity of about 1200 m/s.

In a series of articles by Troshin *et al.* (see, e. g., [6]), charges of lead azide, blasting caps, etc. were used for detonation initiation in 1.6–3.5-meter long tubes of 6–30 mm in diameter with thin wall films and layers of different flammable liquids (petroleum oils, highly viscous lubricants, individual hydrocarbons) and carbon black, and with different oxidant gases (oxygen or oxygen-enriched air) at an initial pressure of 1 to 40 atm. With such strong initiation, a run-up distance of 20–30 tube diameters was shown to be needed for acceleration of arising flame and transition to a detonation. Similar results have been obtained later in [7, 8].

The heterogeneous ‘gas–film’ system has a number of advantages for application in liquid-fueled RDCs and PDCs. First, the ‘gas–film’ sys-

tem exhibits no fuel-rich limit of detonation propagation: detonation was observed in systems with films of almost arbitrary thickness [6]. This weakens the requirements to fuel metering accuracy and enhances stability of the operation process. Second, the ‘gas–film’ system can be in parallel used for active thermal protection of combustor walls by feeding fuel films to heat-stressed regions. Third, in the stratified ‘gas–film’ system, the cumulative area of interface between phases is relatively small as compared to that in liquid fuel sprays and, therefore, the preliminary evaporation of liquid ahead of the traveling detonation front is insignificant, thus preventing various undesired phenomena like premature ignition, etc. Among disadvantages of the ‘gas–film’ system, one could consider the ‘necessity’ of using powerful sources for detonation initiation as stated in the literature. However, careful analysis of the literature indicates the absence of any reference to the attempts of obtaining the DDT in the ‘gas–film’ system at weak ignition with a source generating an initial SW of insignificant intensity.

The objective of this work is to experimentally investigate the possibility and specific features of DDT in the ‘gaseous oxygen–liquid fuel film’ system when using a weak ignition source.

Experimental Setup and Procedure

The experiments were conducted using the setup shown schematically in Fig. 1. Test section 1 is made of a straight 3-meter-long rectangular 54×24 mm channel with polished inner walls. To register pressure waves and reaction fronts, eight pairs of 4-millimeter-diameter ports for PCB 113B24 pressure transducers PT1–PT8 and FD265A photodiodes PD1–PD8 are made equidistantly (400 mm) in eight (1 to 8) measuring sections of the channel along the centerlines of two adjacent walls; the sensors are numbered by the numbers of measuring sections in which they are installed. The film of liquid fuel is always located on the bottom channel wall. Photodiodes PD1–PD8 are installed in the upper channel wall and pressure transducers PT1–PT8 are installed in the side wall at a height of 27 mm above the liquid fuel film.

The 355-millimeter long optical section 4 with a 50×270 mm quartz glass window is attached by one end to the test section. The other end of the optical section is attached to a 60-millimeter long section of fuel

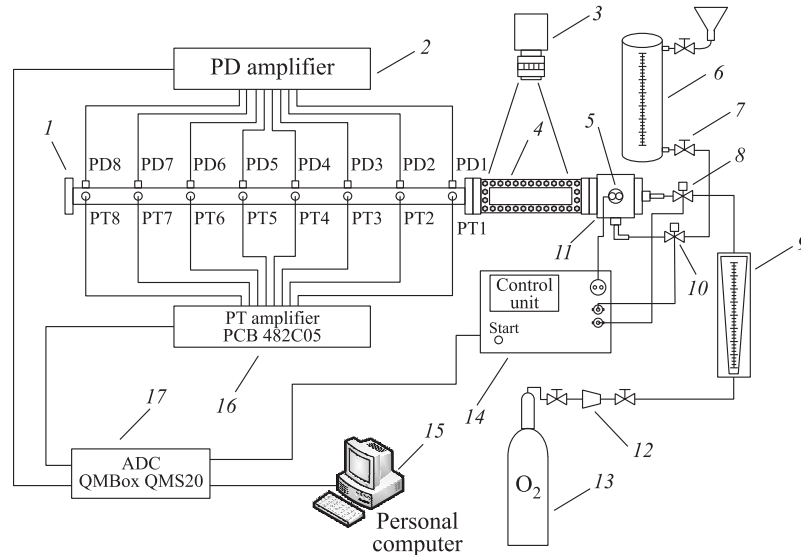


Figure 1 Schematic of the experimental setup

and oxidizer supply 11 with the internal 22×50 mm channel. The opposite side of section 11 is closed by the blind flange. In the middle of section 11, electric discharger 5 is installed. Between the two parallel electrodes of discharger 5, spaced 10 mm apart, a 150-micron-diameter copper wire is fixed. The wire is parallel to the channel axis and is located 13 mm above the liquid fuel film; the distance between the wire and the channel side walls is 11 mm.

Liquid fuel is fed to the channel from fuel tank 6 via the fuel manifold with solenoid valve 10 through five holes located at the bottom of the channel at a distance of 25 mm from the closed end. The fuel tank with a volume of 100 ml is made of organic glass tube 30 mm in diameter, 5 mm thick, and 300 mm long equipped with valves for fuel filling and draining and by valve 7 for fine fuel flow control. Gaseous oxygen is fed into the channel from cylinder 13 through flow controller 12 and flowmeter EMIS-META-210R 9 through a manifold with solenoid valve 8 and a 3-millimeter-diameter orifice located in the center of the closed end. The oxygen flow rate is adjusted by the outlet pressure in

flow controller 12 and by the control valve on flowmeter 9.

Operation of solenoid valves 10 and 8 and blasting of copper wire are controlled by control unit 14 comprising a programmable timer, a power unit, and a capacitor of capacitance $C = 6800 \mu\text{F}$ discharged through the gap of discharger 5. The control unit is used to run the analog-to-digital converter (ADC, R-Technology QMBox QMS20) 17 which is connected with sensors PT1–PT8 and PD1–PD8 through amplifiers 2 and 16. Positions of the sensors in the setup are listed in Table 1. The sampling rate of ADC data is set equal to 600 kHz. Data from ADC 17 are recorded on personal computer 15. In a series of experiments, high-speed video-camera 3 (Phantom Miro LC310) was used for video recording of the explosion process in optical section 4.

Before experiments, the channel was set with a certain slope to the horizon (3.5°) to ensure that liquid fuel is spread over the channel bottom creating a thin film. Further, discharger 5 with copper wire was mounted in section 11, fuel tank 6 was filled with the liquid fuel (*n*-heptane), and the flow rate of fuel was adjusted using valve 7 at open valve 10. The fuel flow rate was calculated based on the change in liquid level in fuel tank 6 during a known time interval. Oxygen flow rate was set up by flowmeter 9 at open valve 8. Control unit 14 was programmed in terms of time intervals. During the first interval lasting 60 to 120 s, the channel was purged with oxygen with the total volume of oxygen exceeding the volume of the channel at least by a factor of ~ 3 . During the second interval lasting 80 s, the channel was purged with oxygen and fuel was supplied for creating a liquid fuel film on the bottom wall. Then, the supply of both oxygen and fuel was terminated by switching off solenoid valves 8 and 10 and simultaneously the control unit issued a command to run ADC 17 and, in 100 ms, a command to burst the copper wire by discharging the capacitor precharged to voltage U . The

Table 1 Distances to sensor positions from the closed end of the channel

Section	Distance without optical section, mm	Distance with optical section, mm
1	170	515
2	570	925
3	970	1325
4	1370	1725
5	1770	2125
6	2170	2525
7	2570	2925
8	2970	3325

energy of discharge (ignition energy) was calculated by the formula $E_i = CU^2/2$.

The mean velocity of liquid fuel inside the channel was estimated based on the time interval the fuel began to leak through the far (open) end of the channel. At the slope angle of the channel equal to 3.5° , the mean velocity of liquid fuel in the wall film was (6 ± 1) cm/s.

The mean fuel flow rate in each experiment was determined based on the height of liquid column in tank 6 before (h_{f0}) and after (h_{f1}) experiment using formula $Q_f = (h_{f0} - h_{f1})\pi/800$ where the flow rate is measured in cm^3/s at the height of the column expressed in mm. Knowing the value of Q_f , one may estimate the mean thickness of the fuel film (in mm) as $\delta_f = 100Q_f/(uw)$ where $w = 24$ mm is the channel width and $u = 6$ cm/s is the mean velocity of liquid fuel in the wall film.

Results and Discussion

The experiments were performed for five different values of ignition energy E_i (from 14 to 480 J) and for three values of oxygen flow velocity during purging, u_{O_2} : 0, 2, and 13 cm/s. The major part of the experiments was performed without optical section.

In the experiments, the DDT in the ‘gas–film’ system at weak ignition was registered apparently for the first time. The term ‘weak ignition’ is used here in the sense that the ignition source (bursting copper wire) generates an initial SW of really insignificant intensity.

Table 2 presents the results of 16 experimental runs in terms of the DDT run-up distance L^* and time T^* , mean detonation velocity D , and the mean Mach number M_0 of an SW generated by the ignition source at the first measuring segment (between measuring sections 1 and 2) at a given ignition energy E_i , the mean velocity of oxygen flow during channel purging, u_{O_2} , and the mean thickness of *n*-heptane film, δ_f . Sign ‘+’ marks the modes of reaction front propagation with the velocity close to the detonation velocity ($D > 1500$ m/s), which exhibit simultaneous sharp deviation of signals recorded by pressure transducers (PT) and photodiodes (PD) mounted in one section of the channel. Sign ‘–’ marks the low-speed modes of reaction front propagation, which exhibit a significant (but steady) time delay of combustion-induced luminescence behind the SW. The run-up distance L^* and time T^* are defined

Table 2 Results of experiments

Run No.	E_i , J	u_{O_2} , cm/s	δ_f , mm	M_0	L^* , cm	T^* , ms	D , m/s	Mode
1	14 ± 1	0	0,5	1,1	100	4,5	1800/980	+/-
2		0	0,5	1,2	96	3,8	1810	+
3		2	0,4	1,1	122	7,5	2060	+
4	27 ± 1	13	0,4	1,0	176	22,5	1875	+
5		13	0,7	1,2	—	—	760	-
6		2	0,4	1,0	196	10,1	1920	+
7		13	0,4	1,0	—	—	740	-
8	52 ± 3	13	0,4	1,0	190	30,7	1700	+
9		13	0,7	1,2	103	3,8	1925	+
10		13	0,7	1,4	100	2,6	1890	+
11		2	0,4	1,4	104	3,5	1970	+
12		13	0,3	1,2	108	4,3	1815	+
13	210 ± 10	13	0,4	1,2	210	7,2	2030	+
14		13	0,4	1,2	110	4,6	1850	+
15		13	0,7	1,4	152	3,5	1930	+
16	480 ± 10	13	0,4	1,4	112	3,6	1870	+

as the coordinates of the point of intersection of the extrapolated lines on an experimental ‘distance–time’ diagram ($x-t$ diagram), depicting the propagation of detonation and retonation waves formed as a result of a secondary explosion (the ‘explosion in the explosion,’ according to Oppenheim). The mean detonation velocity D was determined as the mean value at two or three measuring segments depending on the value of run-up distance L^* .

Figure 2 shows an example of records of pressure transducers PT1–PT8 (solid curves) and photodiodes PD2–PD8 (dashed curves) in Run 2 with an ignition energy of 27 J in the absence of oxygen flow over the fuel film. One can see from the records of sensors PT1–PT4 that the bursting of wire forms a weak (quasi-acoustic) SW propagating at a velocity of about 380 m/s ($M_0 = 1.17$). A slight increase in pressure in this SW is barely noticeable in the relevant records of sensors PT1–PT4 at time instants 0.6, 1.7, 2.7, and 3.8 ms, respectively. The first signs of combustion-induced luminescence appear at time ~ 3 ms in the record of photodiode PD2 without essential pressure raise; the duration of lu-

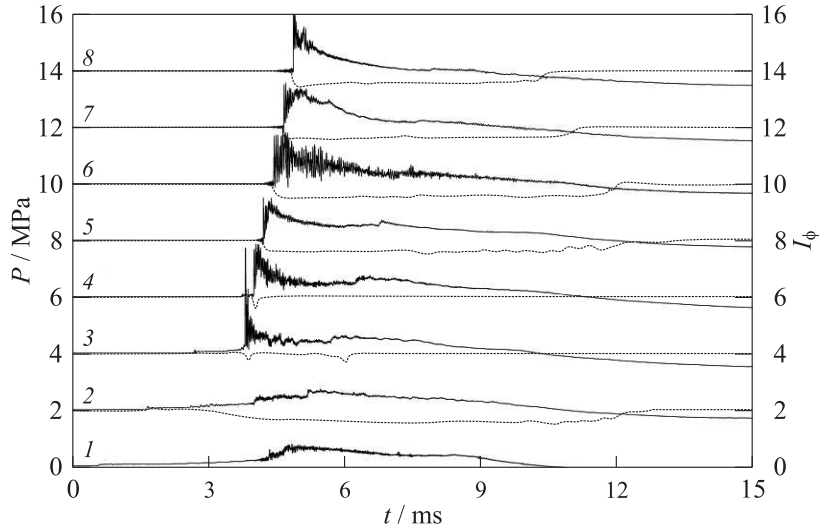


Figure 2 Records of pressure transducers PT (solid lines) and photodiodes PD (dotted lines) in Run 2. Numbers 1 to 8 along the Y-axis correspond to measuring sections 1 to 8

minescence is ~ 10 ms, thus indicating the presence of combustion in measuring section 2. The sharp increase in pressure (up to ~ 3.5 MPa) in phase with luminescence occurs in measuring section 3 located at a distance of 0.97 m from the closed end of the channel. The amplitude of the SW traveling towards the open end of the channel at sensors PT4–PT8 is approximately constant and attains 1.5–1.7 MPa; the signals of photodiodes PD4–PD8 jump together with the signals of the corresponding pressure transducers, i. e., the reaction is initiated by a strong SW.

The SW and reaction front velocities D_{4-5} , D_{5-6} , D_{6-7} and D_{7-8} at the respective measuring segments PT4–PT5 (PD4–PD5), PT5–PT6 (PD5–PD6), PT6–PT7 (PD6–PD7), and PT7–PT8 (PD7–PD8) are approximately equal and attain the mean value of ~ 1810 m/s. The fact that the pressure and luminescence signals in measuring sections 3 to 8 jump together from the zero line and a high level of propagation velocities (above 1500 m/s) of SW and reaction front allows one to treat this

reaction wave as a detonation. The detonation in the ‘gas–film’ system propagates due to rapid mixing of fuel and oxidant behind the leading SW followed by spontaneous ignition of the shock-compressed mixture thus formed. Deflagration-to-detonation transition occurs at distance $L^* \sim 1$ m from the ignition point in time $T^* = 3.8$ ms after ignition. It is worth emphasizing that the luminescence signal at the location of detonation onset has a much shorter duration than in a propagating detonation wave (compare signals of PD4 and PD5 sensors in Fig. 2). Apparently, at the location of DDT, one of the components of the combustible mixture (oxygen or fuel vapor) underwent rapid and complete burnout.

Given the locations of pressure transducers and photodiodes in each measuring section, it can be argued that the detonation front is virtually flat, at least to a height of ~ 27 mm above the fuel film. The thermodynamic calculation of Chapman–Jouguet (CJ) detonation parameters (marked with index CJ) of a homogeneous stoichiometric oxygen–*n*-heptane without considering dissociation gives the following values: propagation velocity $D_{CJ} = 2340$ m/s; pressure $P_{CJ} = 3.9$ MPa; temperature $T_{CJ} = 3860$ K; and sound velocity $a_{CJ} = 1260$ m/s. Based on the calculated value of the sound velocity in the detonation products, it is possible to estimate the frequency of transverse waves with respect to channel width (~ 26 kHz) and height (~ 12 kHz). In Fig. 2, the frequency of pressure pulsations in the detonation front is 24–38 kHz, i. e., correlates with the estimated upper level. However, the measured value of the detonation velocity (~ 1810 m/s) as well as the measured maximum and mean pressure values in the detonation wave in Fig. 2 (~ 1.5 and ~ 1 MPa, respectively) are seen to be significantly lower than the calculated values. The velocity deficit and low pressure of detonation products are apparently caused by various losses due to finite-time mixing, lateral expansion, friction, and heat transfer. In Run 2, the entire process of the combustion is very fast: it lasts for only ~ 5 ms.

Figure 3 shows the x – t diagram of explosion process development in Run 2. Such a diagram is plotted based on the records of sensors PT1–PT8 and PD2–PD8 with the identification of SWs, reaction fronts, detonation, retonation, and rarefaction waves. It is seen from Fig. 3 that after the initial flame acceleration, a secondary explosion occurs (a kink in curve 2 at a distance of ~ 1 m) giving birth to a detonation wave (curves 2 and 3 merge) that catches the quasi-acoustic SW generated

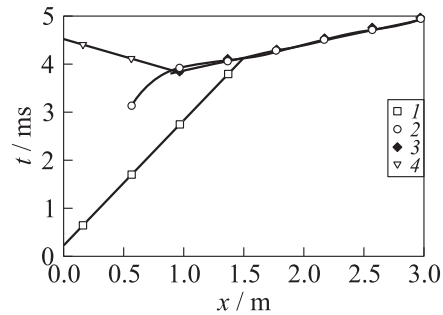


Figure 3 Experimental $x-t$ diagram for Run 2: 1 — weak SW from ignition source; 2 — flame front; 3 — detonation wave; and 4 — retonation wave

that beginning with measuring section 6, there is some lag of the luminescence signal from the shock front. Furthermore, the mean SW velocity at measuring segments PT6–PT7 and PT7–PT8 becomes lower by about 1100–1200 m/s than at segment PT4–PT5: it decreases from $D_{4-5} = 2020$ m/s to $D_{6-7} = 820$ m/s and $D_{7-8} = 860$ m/s. Due to the limited length of the measuring section, one cannot say with certainty whether the observed low-speed (800–900 m/s) mode of reaction wave propagation is stable.

In measuring section 8, the pressure profile behind the SW exhibits a pressure drop followed by the gradual pressure rise till the point at which the luminescence intensity attains its maximum level and thereafter, the pressure gradually decreases. Such a wave structure is typical for reaction fronts propagating in heterogeneous media, when an SW propagating through the gas first induces the interphase mass, momentum, and energy exchange between phases causing explosive mixture formation and then induces ignition and energy release; the duration of the shock-induced energy release depends on combustion macrokinetics including the rates of various physical and chemical processes. When comparing the pressure and luminescence records in Fig. 4, one can see that the ignition delay in measuring section 8 is approximately 120 μ s. During this time interval, the leading shock front travels a distance of about 10 cm providing mixture formation in the initially stratified sys-

by the ignition source (curve 1).

In Run 1 (see Table 2), with the smaller ignition energy (14 J) than in Run 2 (27 J), an interesting phenomenon was detected: a high-speed detonation-like combustion wave was transformed after a while to a low-speed combustion wave composed of the leading SW followed by the separated reaction front (Fig. 4). As a matter of fact, one can see in Fig. 4

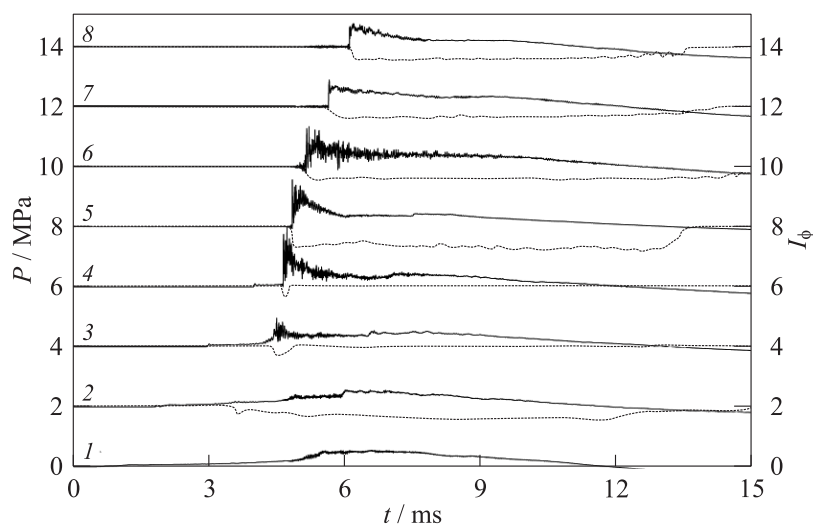


Figure 4 Records of pressure transducers (solid lines) and photodiodes (dotted lines) in Run 1. Numbers 1 to 8 along the Y-axis correspond to measuring sections 1 to 8

tem. Further investigations are needed to understand the reason why the high-speed detonation mode in Run 1 is suddenly transformed to the low-speed combustion mode.

In other experiments with the ignition energy of 27 J and in experiments with $E_i = 52$ J (see Table 2), the DDT with both relatively short and long run-up time was observed without transformation of the high-speed detonation mode to the low-speed combustion mode (see, e. g., Runs 4 and 8 in Table 2). In some runs with such ignition energy (see, e. g., Runs 5 and 7), only low-speed combustion mode was observed. In other words, the DDT run-up time and distance were somewhat changing from one run to another.

In experiments with relatively large ignition energy (210 J), the DDT run-up distance and time also changed from run to run. Thus, in Runs 12 and 13, the DDT run-up distances were $L^* \sim 1.1$ and 2.1 m, respectively, although the experimental conditions were apparently the same and the difference in fuel film thickness was within its measurement error. In fact, to determine the actual film thickness is very dif-

difficult even with precise measurements of flow rates because the exact value of wetted surface area is unknown due to capillary effects and partial ablation of fuel with oxygen flow during purging.

The differences in the measured values of the DDT run-up distance and time may be associated with the stochastic nature of the DDT phenomenon in the stratified ‘gas–film’ system. However, despite the differences in the dynamics of explosion, the measured propagation velocities of the detonation-like waves in all runs are close to each other and the pressure and luminosity profiles in these waves look the same and retain their shape. Moreover, the propagation velocity and structure of such waves are essentially independent of the ignition energy.

Analysis of videoframes of the DDT process showed that the combustion develops in the channel in a relatively thin layer over the fuel film and even at relatively long times after ignition (1–2 ms), the combustion zone occupies only a part of channel cross section. Uniform luminescence across the channel height has been observed only behind a detonation wave.

Concluding Remarks

Deflagration-to-detonation transition in a channel with a thin film of liquid fuel on the wall and gaseous oxidizer in the volume has been obtained experimentally apparently for the first time using a weak ignition source, which generates the initial SW of insignificant intensity.

In a series of experiments with different ignition energy (14 to 480 J) in a straight 3-meter long channel of rectangular cross section 54×24 mm with smooth internal walls and with one open end, the DDT in the ‘gas (oxygen)–liquid fuel (*n*-heptane) film’ system was detected at run-up distances of 1 to 2 m from the ignition source and run-up time of 3.4 to 30 ms after ignition.

Despite some differences in the dynamics of the DDT from run to run with both different and similar ignition energies, the measured propagation velocity of the arising detonation waves was 1800–2000 m/s (77%–85% of the CJ detonation velocity) and did not depend on the ignition energy, whereas the measured pressure and combustion-induced luminescence profiles in the detonation wave retained their shape.

High-speed video recording at the initial section of the channel showed that combustion develops in a relatively thin layer over the

liquid film even at a relatively large time after ignition comparable to the DDT run-up time.

In some experiments, a quasi-stationary low-speed detonation-like combustion front, traveling at an average velocity of 700–900 m/s was detected. The structure of such reaction waves is shown to include a leading SW followed by a reaction zone separated by a time delay of 80 to 150 μ s. The results obtained can be used for improving the operation process in PDCs and RDCs.

Acknowledgments

This work was supported by the Russian Foundation for Basic Research (grants 15-08-00782 and 16-29-01065) and Russian Science Foundation (grant 14-13-00082).

References

1. Roy, G. D., S. M. Frolov, A. A. Borisov, and D. W. Netzer. 2004. Pulse detonation propulsion: Challenges, current status, and future perspective. *Prog. Energ. Combust. Sci.* 30(6):545–672.
2. Voitsekhovskii, B. V. 1959. Stacionarnaya detonatsiya [Stationary detonation]. *Dokl. Akad. Nauk SSSR* 129(6):1254–1256.
3. Frolov, S. M., A. E. Zangiev, V. S. Ivanov, and K. A. Avdeev. 01.08.2013. Vozdushno-reaktivnyy impul'snyy detonatsionnyy dvigatel' (varianty) [Air-breathing pulse detonation engine (variants)]. PCT Patent application PCT/RU2013/000663.
4. Frolov, S. M. 16.10.2014. Sposoby organizatsii rabocheho protsessa v nepreryvno-detonatsionnoy kamere sgoraniya reaktivnogo dvigatelya na zhidkom toplive i ustroystva dlya ikh osushchestvleniya [Methods of arranging operation process in continuous-detonation combustor of liquid-fueled jet engine and device for its realization]. PCT Patent application PCT/RU2014/000779.
5. Loison, R. 1952. The propagation of deflagration in a tube covered with an oil film. *Comptes Rendus* 234(5):512–513.
6. Komov, V. F, and Ya. K. Troshin. 1967. O svoystvakh detonatsii v nekotorykh geterogennykh sistemakh [On the properties of detonation in some heterogeneous systems]. *Dokl. Akad. Nauk SSSR* 175(1):109–112.
7. Ragland, K. W., and J. A. Nicholls. 1969. Two-phase detonation of a liquid layer. *AIAA J.* 7(5):859–863.
8. Sichel, M., C. S. Rao, and J. A. Nicholls. 1971. A simple theory for the propagation of film detonations. *Proc. Combust. Inst.* 13:1141–1149.